ELSEVIER

www.elsevier.nl/locate/jorganchem

Journal of Organometallic Chemistry 588 (1999) 113–124

Journal of Organometallic Chemistry

Synthesis, structural characterisation and electrochemistry of ruthenium carbonyl clusters derived from ferrocenyl(formyl)acetylene

Cindy Sze-Wai Lau, Wing-Tak Wong *

Department of Chemistry, The University of Hong Kong, Pokfulam Road, Hong Kong, PR China

Received 5 May 1999

Abstract

Two new ferrocenyl ruthenium carbonyl clusters, $[Ru_4(CO)_{12}(\mu_4\text{-}\eta^1,\eta^1,\eta^2,\eta^2\text{-}\{(C_5H_5)Fe(C_5H_4CCCHO)\})]$ **1** (20%) and $[Ru_3(CO)_8(\mu_3\text{-}\eta^1,\eta^2,\eta^4\text{-}\{(C_5H_5)Fe(C_5H_4CCCHO)\}_2)]$ **2** (10%), have been synthesised by reaction of $(C_5H_5)Fe(C_5H_4C\equiv CCHO)$ with triruthenium dodecacarbonyl in cyclohexane under refluxing conditions. Thermolysis of **1** in refluxing toluene led to the formation of $[Ru_5(CO)_{13}(\mu\text{-}H)(\mu_5\text{-}C)(\mu_2\text{-}\eta^1,\eta^1\text{-}\{(C_5H_5)Fe(C_5H_4C)\})]$ **3** (10%). Reaction of $[Ru_3(CO)_{10}(NCMe)_2]$ with ferrocenyl-(formyl)acetylene afforded the triruthenium cluster $[Ru_3(CO)_9(\mu\text{-}CO)(\mu_3\text{-}\eta^1,\eta^1,\eta^2\text{-}\{(C_5H_5)Fe(C_5H_4CCCHO)\})]$ **4** (30%). All these new compounds have been characterised fully by conventional spectroscopic and X-ray diffraction methods. The structure of **1** consists of a ferrocenyl carboxaldehyde bound to the Ru_4 butterfly skeleton via a typical $\mu_4\text{-}\eta^1$, η^1, η^2, η^2 coordination mode. Cluster **2** is based upon an Ru_3 closed triangle bearing a metallacyclopentadiene ring that arises from the coupling of two ligand molecules with the formation of $O\rightarrow Ru$ dative bond. Thermolysis of **1** afforded a rare pentanuclear ruthenium cluster containing a carboferrocenyl fragment with a $\mu_2\text{-}\eta^1,\eta^1$ mode. Both fluxional and electrochemical behaviour of cluster **3** have been studied. Compound **4** consists of an alkyne ligand bound to the triruthenium cluster unit via a typical $\mu_3\text{-}(\eta^2\text{-}\|)$ coordination mode.

Keywords: Ferrocenyl; Ruthenium; Carbonyl; Clusters

1. Introduction

The chemistry of ferrocenyl transition-metal complexes has attracted a great deal of interest. A number of transition metal complexes containing ferrocene have been synthesized, but in most of them transition-metal atoms were linked to ferrocene by heteroatoms such as nitrogen, oxygen and phosphorus [1–4]. Alkyne and alkynyl species bearing a C≡C functional group belong to a class of surface species which may play pivotal role in various catalytic reactions such as CO hydrogenation (Fischer–Tropsch process) [5,6]. Therefore, alkyne-bridged di- or polynuclear metal carbonyls could serve as model compounds in heterogeneous catalysis. A ligand bonded to a metal cluster can simulate the adsorption of the same species on a metal surface, and show interesting alkyne-bridged ligand rearrangements [7] and diastereoselective transformations [8,9] on tri- or tetra-metallic clusters. In order to access this class of compounds, we have been developing strategies for the synthesis of functionalized-alkyne clusters [10,11]. Our recent work has focused on the ferrocenyl derivatives due to its importance in electroactive hetero-polynuclear aggregates [12] and as donors in charge-transfer complexes [13]. Moreover, transition-metal clusters have been shown to possess interesting magnetic [14] and redox properties [15]. The idea of combining the properties of these two sets of fascinating molecules has significant appeal. However, reports on the ferrocenylacetylenic cluster compounds are relatively rare. Some examples are the mononuclear complex $[PtH(C\equiv CFc)(PPh_3)_2]$ [16], the dinuclear complex $[Ru_2(CO)_6(C_4H_2Fc)_2]$ [17], and the trinuclear complexes such as $[Co_3(CO)_9(CC\equiv CFc)]$ [18] and $[Os_3H(CO)_{10}(CH{=}CHFc)]$ [19] (where $Fc{=}C_5H_5$-

* Corresponding author. Fax: +86-852-25472933.
E-mail address: wtwong@hkucc.hku.hk (W.-T. Wong)

0022-328X/99/$ - see front matter
PII: S0022-328X(99)00353-8

FeC_5H_4). Deeming and co-workers [20] have described the reactions of $[Os_3(CO)_{10}(NCMe)_2]$ with ethynylferrocene $[(C_5H_5)FeC_5H_4CCH]$, where the ethynylferrocene coordinates to the triosmium metal core based upon a C≡C triple bond activation, which leads to the formation of $[Os_3(CO)_{10}(FcCCH)]$ with a μ_3-η^1,η^1,η^1 bonding mode. This will rearrange to $[Os_3H(CO)_9$-(FcCC)]with a μ_3-η^1,η^2,η^2 mode under a thermolytic reaction. We describe here the preparation and spectroscopic studies of four new clusters that were obtained by the reaction of triruthenium clusters with ferrocenyl(formyl)acetylene, which involves C≡C triple bond activation and C–C coupling. All of these products were investigated by electrochemical analysis and UV–vis spectroscopic studies.

2. Results and discussion

The reaction of $[Ru_3(CO)_{12}]$ with ferrocenyl-(formyl)acetylene in refluxing cyclohexane (80°C) under a dinitrogen atmosphere generated two compounds in relatively low yields. These were separated by preparative thin-layer chromatography (TLC). Two new compounds were isolated and identified as $[Ru_4(CO)_{12}$-$(\mu_4$-η^1,η^1,η^2,η^2-{$(C_5H_5)Fe(C_5H_4CCCHO)$}$)]$ **1** and $[Ru_3(CO)_8(\mu_3$-η^1,η^2,η^4-{$(C_5H_5)Fe(C_5H_4CCCHO)$}$_2)]$ **2** in 20 and 10% yields, respectively [based on $Ru_3(CO)_{12}$]. Thermolysis of **1** led to the formation of $[Ru_5(CO)_{13}(\mu$-H$)(\mu_5$-C$)(\mu_2$-η^1,η^1-{$(C_5H_5)Fe(C_5H_4C)$}$)]$ **3** (10%). Reaction of $[Ru_3(CO)_{10}(NCMe)_2]$ with ferrocenyl(formyl)acetylene afforded the triruthenium cluster $[Ru_3(CO)_9(\mu$ - CO$)(\mu_3$ - η^1,η^1,η^2 - {$(C_5H_5)Fe(C_5H_4CCC$-HO$)$}$)]$ **4** (30%) and **1** (8%) (Scheme 1). All the compounds were characterized fully by FAB mass spectrometry, IR and ^{1}H-NMR spectroscopies and single-crystal X-ray crystallography. The structure of compound **3** was also elucidated by the variable-temperature ^{1}H-NMR technique.

2.1. Treatment of $[Ru_3(CO)_{12}]$ with ferrocenyl(formyl)acetylene

The chromatographic separation of the reaction mixture in the first fraction yielded brown crystals of **1** after recrystallization. Its positive FAB mass spectrum shows a parent molecular ion peak at m/z 979, which is consistent with 12 terminal carbonyl ligands and one

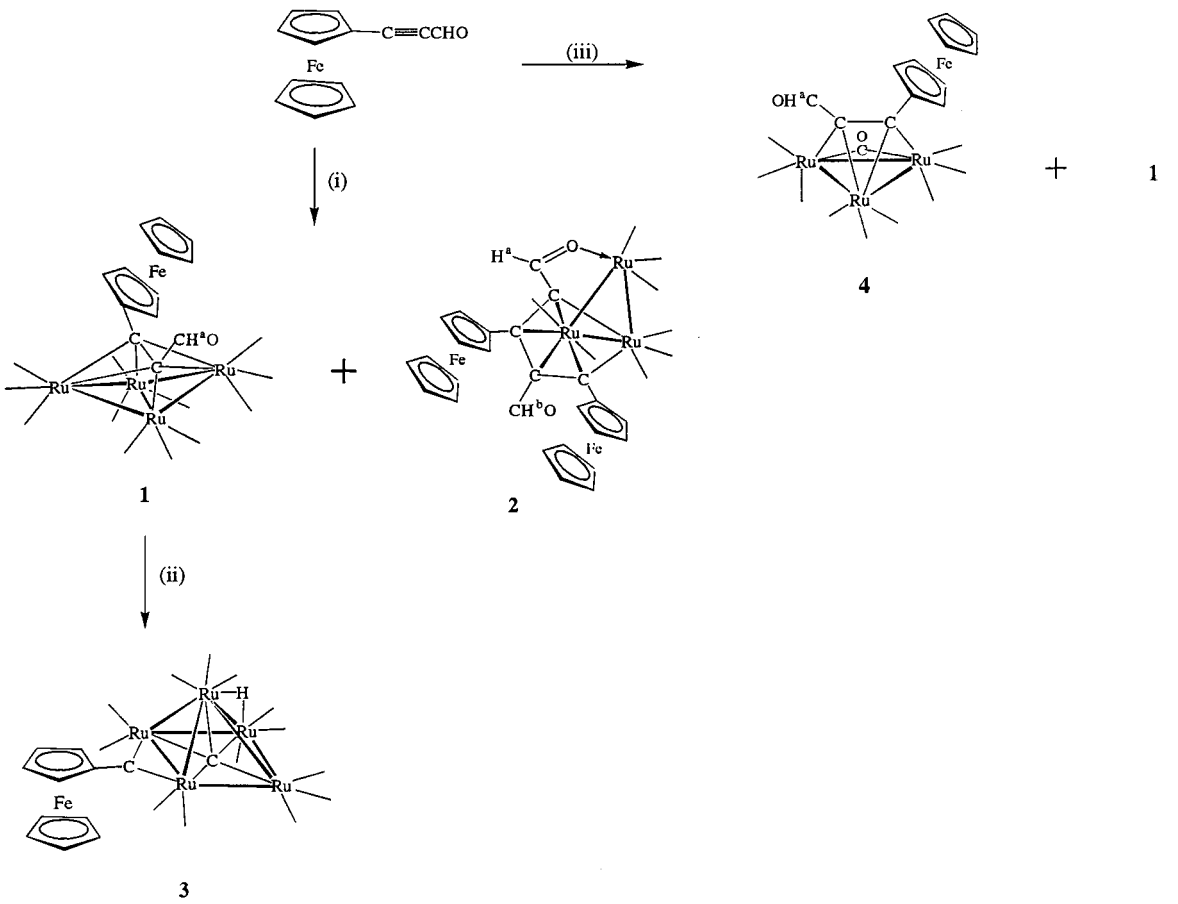

Scheme 1. (i) $[Ru_3(CO)_{12}]$ in refluxing cyclohexane for 45 min. (ii) Under toluene reflux for 8 h. (iii) $[Ru_3(CO)_{10}(NCMe)_2]$ in CH_2Cl_2 stirred at r.t.

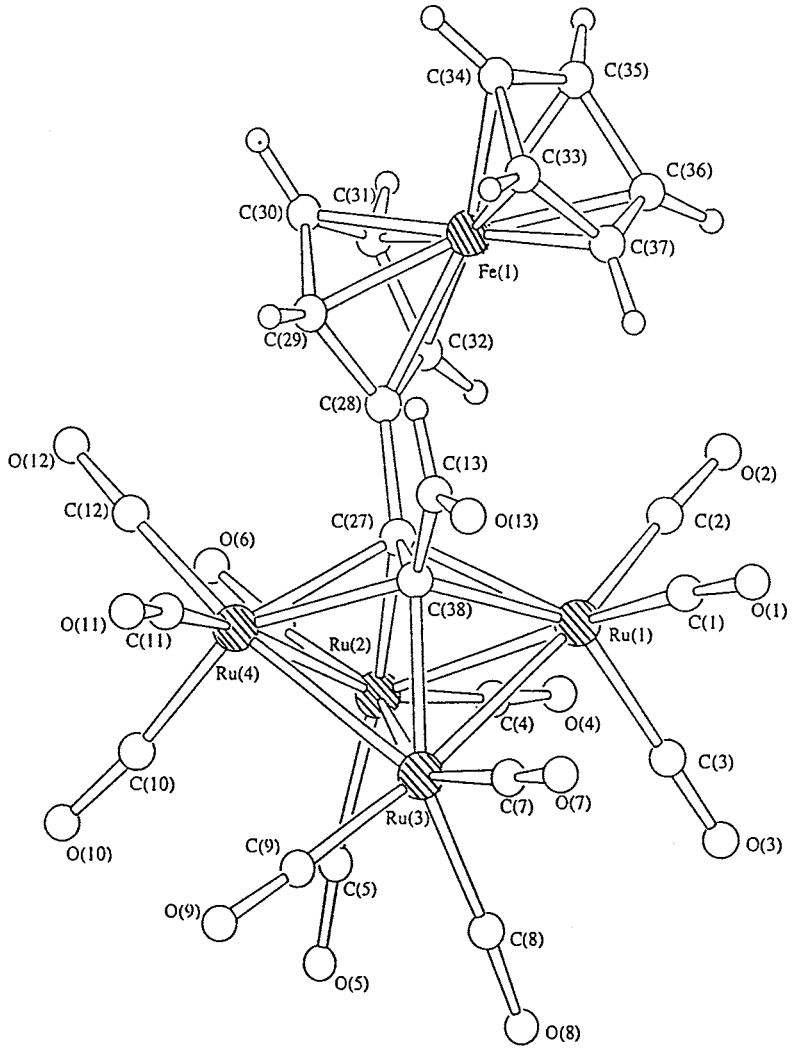

Fig. 1. Molecular structure of cluster **1**.

ligated olefinic fragment. The ^{1}H-NMR spectrum of **1** in $CDCl_3$ exhibits a signal at δ 10.87, which is attributed to the aldehyde proton. In addition, a single resonance due to protons of the C_5H_5 ring is observed at δ 4.17, while two triplet signals are observed in the range δ 4.22–4.31 due to the C_5H_4 ring protons. Moreover, the IR spectrum reveals the presence of terminal carbonyl ligands only (see Table 5). An X-ray structural analysis was undertaken and a perspective view is shown in Fig. 1 together with the atomic numbering scheme. The asymmetric unit consists of two independent but structurally similar molecules of **1**. The selected bond parameters are presented in Table 1. The four ruthenium atoms adopt a butterfly configuration, while the ferrocenyl(formyl) acetylenic moiety lies over the metal skeleton with the ethylenic C–C bond parallel to the Ru–Ru hinge bond. The ligand capped on the butterfly framework is different from those observed in $[Ru_4H(CO)_{12}\{C{\equiv}C(C_5H_4)Fe(C_5H_5)\}]$ [21], which is a μ_4-$\eta^1,\eta^1,\eta^1,\eta^2$ coordination mode. Each acetylenic carbon atom of the organic fragment forms two σ-bonds with the hinge ruthenium atoms [Ru(2)–C(27) 2.09(2) Å, Ru(3)–C(38) 2.13(2) Å] and two π-bonds with the wingtip atoms [average Ru(1)–C 2.22(2) Å and Ru(4)–C 2.24(2) Å] to form a distorted octahedral core. The dihedral angle formed by the two butterfly wings is 115.3°. Similar types of clusters with analogous M_4C_2 frameworks have been structurally characterised [22,23]. Compound **1** has an electron count of 62 CVE in which the organic fragment donates six electrons toward skeletal bonding.

The second product **2** was observed as a black band and was isolated as an oily material. The IR spectrum of compound **2** in the carbonyl region indicated the presence of terminal CO groups only (Table 5). The positive FAB mass spectrum showed an envelope with a molecular ion peak at m/z 1004. The ^{1}H-NMR spectrum recorded in $CDCl_3$ showed two downfield singlets at δ 11.27 and 10.94, indicative of two aldehyde protons. Again, two single resonances at δ 4.24 and 4.09

were observed, which may be assigned to the two unsubstituted cyclopentadienyl rings of the ferrocene groups. The protons of the substituent-bearing cyclopentadienyl rings gave rise to a complicated multiplet in the regions δ 4.11–4.21 and δ 4.26–4.56, respectively. It is obviously noted that the two ferrocenyl(formyl)acetylene groups coordinated to the Ru_3 core are nonequivalent. One set of more downfield signals may be assigned as the ferrocene group of Fe(1) due to its stronger electron-withdrawing ability than the second ferrocene group. Due to the relative instability of compound **2** in solution, crystals suitable for X-ray analysis were obtained with great difficulty. We were fortunate to isolate a stable black crystal, which turned out to contain compound **2** with a solvent molecule of CH_2Cl_2 in the asymmetric unit. A perspective drawing of cluster **2** with the atomic numbering scheme is shown in Fig. 2. Selected interatomic bonds and angles are listed in Table 2. The molecular structure of **2** features the Ru_3 closed triangular metal core bonded with eight terminal CO groups. The Ru–Ru bond lengths lie in the range of 2.702(3)–2.822(3) Å; nearly equal bond angles were observed for Ru(2)–Ru(1)–Ru(3), 58.8(6)°, and Ru(2)–Ru(3)–Ru(1), 58.4(6)°, and a slightly larger angle was found for Ru(1)–Ru(2)–Ru(3), 62.80(7)°. Two acetylenic carbons, C(10) and C(22), bridged to the Ru(2)–Ru(3) edge, lead to the formation of two butterflies. The dihedral angles of the two pairs of butterfly wings Ru(1)–Ru(2)–Ru(3)/Ru(2)–C(10)–Ru(3) and Ru(1)–Ru(2)–Ru(3)/Ru(2)–C(22)–Ru(3) were 89.6 and 169.3°, respectively. A remarkable feature of the structure of **2** lies in the resulting ligand, which was derived from the head-to-tail coupling of two ferrocenyl(formyl) acetylene ligands, to afford an unusual μ_3-η^1,η^2,η^4 coordination mode. This is found to be in contrast to those observed in $[Cp^*Ru\{\mu_2\text{-}\eta^1,\eta^2\text{-}C(=CHFc)C{\equiv}CFc\}(\mu_2\text{-}SPr^i)_2RuCp^*]^+$ [24] and $[Os_3(CO)_9\{(FcCCH)_2CO\}]$ [25], bearing head-to-head coupling of two HC≡CFc molecules. This gives rise to a ruthenole unit formed from the π coordination of the ruthenacyclopentadiene ring Ru(3)–C(10)–C(11)–C(33)–C(22) to Ru(2), with carbon–carbon bond lengths within this C_4 fragment [C(10)–C(11) 1.45(3) Å, C(11)–C(33) 1.41(3) Å, C(22)–C(33) 1.46(3) Å] suggestive of limited delocalization over the C_4 unit [26,27]. It is noteworthy that the three C–C π bonds in **2** are slightly longer than for other Group VIII metallacyclopentadiene rings [28–30], which may be due to the greater steric requirement of the ferrocenyl group. Moreover, two ferrocenyl groups are bonded to the metallacyclopentadiene ring via a C≡C triple bond activation, forming one long [C(11)–C(12) 1.53(3) Å], and one short [C(22)–C(23) 1.46(3) Å] C–C single bond. Another interesting feature in this compound was the activation of a C=O bond in one of the aldehyde groups, which was then coordinated to the Ru(1) atom. The Ru(1)–O(9) distance [2.19(1) Å] is typical of an O→Ru dative bond observed in the related clusters $[Ru_5(\mu_5\text{-}C)(CO)_{13}\{C_2H_2(CO_2Me)_2\}]$ [31] and $[Ru_5(\mu\text{-}Br)(\mu\text{-}PPh_2)_2(CO)_{10}\{\mu_5\text{-}CCC(O)CH_2CH{=}CH_2\}]$ [32]. It is also found that the Ru(1)–O(9)–C(9)–C(10)–Ru(2) fragment forms a dimetallated five-membered ring. Taking into account that triruthenium carbonyl clusters have a closed triangular metal core possessing a typical 48 CVE, we expect that the organic moiety in compound **2** acts as an eight-electron donor.

Table 1
Some selected bond lengths (Å) and angles (°) for cluster **1**

Bond lengths (Å)			
Ru(1)–Ru(2)	2.766(3)	Ru(1)–Ru(3)	2.709(3)
Ru(2)–Ru(3)	2.850(3)	Ru(2)–Ru(4)	2.717(2)
Ru(3)–Ru(4)	2.741(3)	Ru(1)–C(27)	2.24(2)
Ru(1)–C(38)	2.20(2)	Ru(2)–C(27)	2.09(2)
Ru(3)–C(38)	2.13(2)	Ru(4)–C(27)	2.29(2)
Ru(4)–C(38)	2.19(2)	Fe(1)–C(28)	2.07(2)
Fe(1)–C(29)	2.02(2)	Fe(1)–C(30)	2.00(2)
Fe(1)–C(31)	2.03(2)	Fe(1)–C(32)	2.09(2)
Fe(1)–C(33)	2.04(3)	Fe(1)–C(34)	1.98(3)
Fe(1)–C(35)	2.02(3)	Fe(1)–C(36)	2.03(3)
Fe(1)–C(37)	1.96(3)	C(13)–O(13)	1.19(2)
C(13)–C(38)	1.51(3)	C(27)–C(28)	1.50(3)
C(27)–C(38)	1.45(3)	C(28)–C(29)	1.40(3)
C(28)–C(32)	1.54(3)	C(29)–C(30)	1.42(3)
C(30)–C(31)	1.35(3)	C(31)–C(32)	1.37(3)
C(33)–C(34)	1.38(4)	C(33)–C(37)	1.36(3)
C(34)–C(35)	1.35(4)	C(35)–C(36)	1.43(4)
C(36)–C(37)	1.29(4)		
Bond angles (°)			
Ru(1)–Ru(3)–Ru(2)	59.62(6)	Ru(1)–Ru(2)–Ru(3)	57.65(6)
Ru(2)–Ru(3)–Ru(4)	58.12(6)	Ru(2)–Ru(1)–Ru(3)	62.73(7)
Ru(3)–Ru(2)–Ru(4)	58.94(6)	Ru(2)–Ru(4)–Ru(3)	62.94(7)
C(28)–C(27)–C(38)	123(1)	C(13)–C(38)–C(27)	123(1)

2.2. Thermolysis of compound *1*

Cluster **1** was refluxed in toluene for 8 h to yield three products. The new component was recrystallised from a dichloromethane–*n*-hexane solution to afford dark violet crystals of $[Ru_5(CO)_{13}(\mu\text{-}H)(\mu_5\text{-}C)(\mu_2\text{-}\eta^1,\eta^1\text{-}\{C(C_5H_5)Fe(C_5H_4C)\})]$ **3**. The other products were found to be the known cluster $[Ru_3(CO)_{12}]$ (5%) and $[Ru_6C(CO)_{14}(\mu\text{-}\eta^6\text{-}C_6H_5CH_3)]$ [33] (6%), respectively. A small amount of the unreacted cluster **1** was also recovered. The positive FAB mass spectrum of **3** gives a parent peak at m/z 1080. Following the parent ion, successive carbonyl eliminations typical of carbonyl clusters was observed (Table 5). The ^{1}H-NMR spectrum recorded in $CDCl_3$ at room temperature comprises a broad single hydride signal at δ −21.39 and three successively broadened signals for the ferrocenyl group at δ 4.34, 5.27 and 5.41. The spectrum of com-

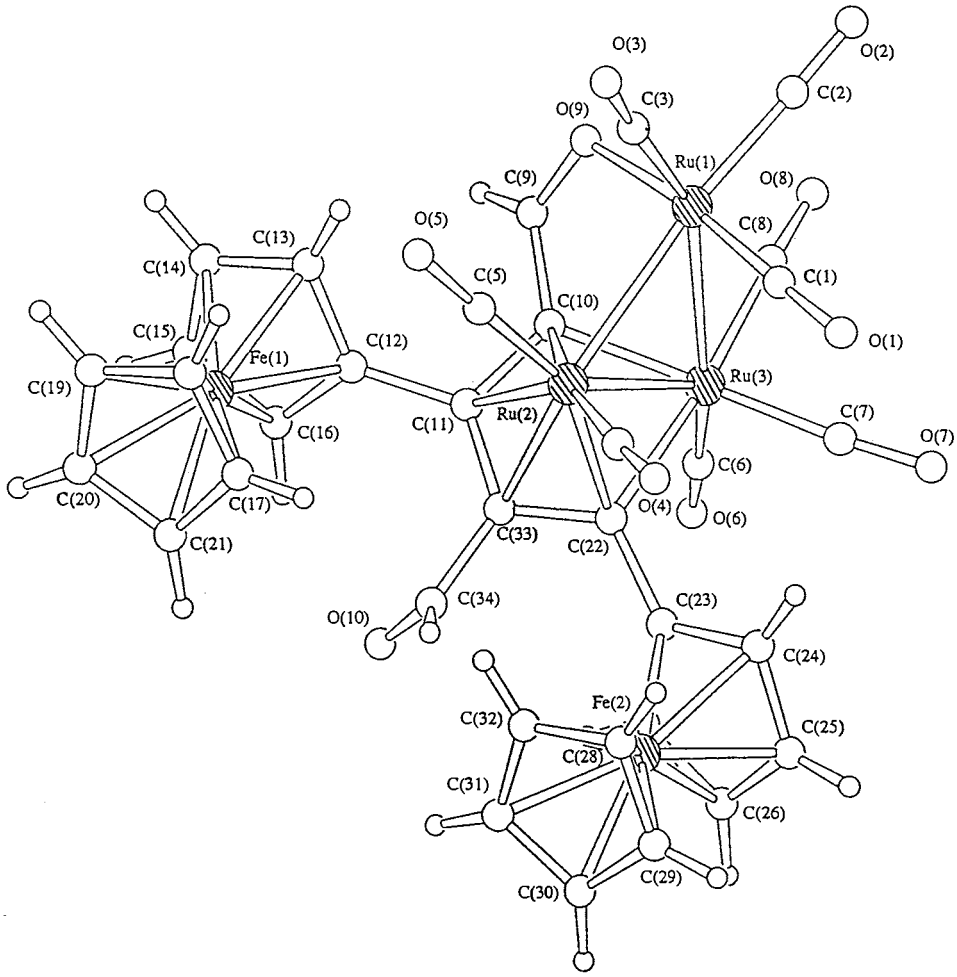

Fig. 2. Molecular structure of cluster **2**.

pound **3** at room temperature is indicative of some kind of fluxional process, which was confirmed by recording spectra over a range of temperatures. These results will be discussed later in this paper. Fig. 3 depicts the molecular structure of cluster **3** together with its important bond parameters shown in Table 3. The core geometry of cluster **3**, which can be described as a distorted square-based pyramid, is similar to that observed in several examples such as $[Ru_5(\mu\text{-}H)(\mu_5\text{-}C)(CO)_{12}(dppe)]$ [34], $[Ru_5(\mu\text{-}H)(\mu_5\text{-}C)(CO)_{13}(\mu\text{-}PPh_2)]$ [35] and $[Ru_5(\mu\text{-}H)(\mu_5\text{-}C)(CO)_{12}(\mu\text{-}SEt)(PPh_3)]$ [36]. The Ru(basal)–Ru(basal) bonds in **3** [average 2.839(5) Å] are shorter than the Ru(apical)–Ru(apical) bonds [average 2.874(5) Å], where the shortest Ru(4)–Ru(5) bond [2.640(2) Å] may reflect the presence of electron unsaturation [37,38]. The hydride ligand was located directly from the difference Fourier technique based on low angle data which is bridging the Ru(1)–Ru(3) edge. The average Ru–C(carbide) distance is 2.04(4) Å, where the Ru(1)–C(14) bond is the longest and the Ru(2)–C(14) bond is the shortest. The carbide atom, C(14), lies 0.11 Å below the Ru_4 square base. The 13 carbonyl groups are effectively linear with an average Ru–C–O angle of 178°. The Ru(4)–Ru(5) edge is bridged by the ferrocenyl alkylidene fragment via two σ bonds. It is noticeable that the bond lengths Ru(4)–C(15) [1.95(2) Å] and Ru(5)–C(15) [1.99(1) Å] are significantly shorter compared with the other Ru–C σ-bond, indicating that there is a delocalization over the Ru(4)–Ru(5)–C(15) triangle. The dihedral angles between the Ru(4)–Ru(5)–C(15)–C(16) plane and the adjacent substituted cyclopentadienyl ring and between Ru(4)–Ru(5)–C(15)–C(16) and Ru(2)–Ru(3)–Ru(4)–Ru(5) planes are 3.1 and 6.4°, respectively. The three planes [Ru(2)–Ru(3)–Ru(4)–Ru(5)], [Ru(4)–Ru(5)–C(15)–C(16)] and [C(16)–C(17)–C(18)–C(19)–C(20)] slightly deviate from co-planarity (maximum deviation 0.41 Å).

When a $CDCl_3$ solution of compound **3** was cooled to −60°C, the rate of the fluxional process was reduced and the two upfield singlet signals observed at δ −21.66 and −21.40 may be assigned as two hydride ligands. Two singlets at δ 4.59 and 4.22, with a relative intensity of 1:1, correspond to the two unsubstituted

cyclopentadienyl rings. A complex multiplet is observed in the range δ 5.15 − 5.53 due to the protons of the two substituted cyclopentadienyl rings. Warming of this solution to − 20°C led to broadening of the resonances of the protons from the two substituted cyclopentadienyl rings, two unsubstituted cyclopentadienyl rings and the two hydrides, respectively. Finally, at 20°C, resonances for the two sets of substituted and unsubstituted cyclpentadienyl rings and hydrides coalesce to give the weighted average of chemical shifts. The consequence of these exchanges in the ^{1}H-NMR spectra implies that there is another isomer which is exchanging rapidly at 20°C but only slowly at very low temperature (− 60°C). One possible isomerization process is the hydride migration on the Ru_5 surface (Scheme 2). The coordination site of the bridging hydride is more likely to be with the Ru(2)–Ru(3) edge rather than the other Ru(basal)–Ru(basal) edges. It is conceivable that the insertion of a hydride to either the Ru(2)–Ru(5) or the Ru(3)–Ru(4) edge pushes CO ligands towards the bulky ferrocenyl group, giving rise to an unfavourable steric hindrance.

Table 2
Some selected bond lengths (Å) and angles (°) for cluster **2**

Bond lengths (Å)			
Ru(1)–Ru(2)	2.701(2)	Ru(1)–Ru(3)	2.822(2)
Ru(2)–Ru(3)	2.713(2)	Ru(1)–O(9)	2.18(1)
Ru(2)–C(10)	2.19(2)	Ru(2)–C(11)	2.31(2)
Ru(2)–C(22)	2.16(2)	Ru(2)–C(33)	2.33(2)
Ru(3)–C(10)	2.09(2)	Ru(3)–C(22)	2.18(2)
Fe(1)–C(12)	2.05(2)	Fe(1)–C(13)	2.05(2)
Fe(1)–C(14)	2.05(2)	Fe(1)–C(15)	2.06(2)
Fe(1)–C(16)	2.03(2)	Fe(1)–C(17)	2.07(2)
Fe(1)–C(18)	2.05(2)	Fe(1)–C(19)	2.04(2)
Fe(1)–C(20)	2.03(2)	Fe(1)–C(21)	2.05(2)
Fe(2)–C(23)	2.06(2)	Fe(2)–C(24)	2.06(2)
Fe(2)–C(25)	2.04(2)	Fe(2)–C(26)	2.05(2)
Fe(2)–C(27)	2.03(2)	Fe(2)–C(28)	2.04(2)
Fe(2)–C(29)	2.06(2)	Fe(2)–C(30)	2.02(2)
Fe(2)–C(31)	2.06(2)	Fe(2)–C(32)	2.03(2)
C(9)–O(9)	1.25(2)	C(9)–C(10)	1.42(3)
C(10)–C(11)	1.45(3)	C(11)–C(12)	1.51(3)
C(11)–C(33)	1.41(3)	C(12)–C(13)	1.40(3)
C(12)–C(16)	1.42(3)	C(13)–C(14)	1.40(3)
C(14)–C(15)	1.38(3)	C(15)–C(16)	1.42(3)
C(17)–C(18)	1.39(3)	C(17)–C(21)	1.37(3)
C(18)–C(19)	1.40(4)	C(19)–C(20)	1.39(4)
C(20)–C(21)	1.40(4)	C(22)–C(23)	1.48(3)
C(22)–C(33)	1.46(3)	C(23)–C(24)	1.44(3)
C(23)–C(27)	1.45(3)	C(24)–C(25)	1.41(3)
C(25)–C(26)	1.42(3)	C(26)–C(27)	1.43(3)
C(28)–C(29)	1.41(3)	C(28)–C(32)	1.41(3)
C(29)–C(30)	1.36(3)	C(30)–C(31)	1.43(4)
C(31)–C(32)	1.35(3)	C(33)–C(34)	1.47(3)
Bond angles (°)			
Ru(1)–Ru(2)–Ru(3)	62.8(6)	Ru(1)–Ru(3)–Ru(2)	58.4(6)
Ru(2)–Ru(1)–Ru(3)	58.8(6)	C(10)–Ru(3)–C(22)	74.5(8)

2.3. Reaction of $[Ru_3(CO)_{10}(NCMe)_2]$ with ferrocenyl(formyl)acetylene

A dichloromethane solution of $[Ru_3(CO)_{10}(NCMe)_2]$ was stirred at room temperature with one molar equivalent of ferrocenyl(formyl)acetylene. This resulted in a dark red solution and subsequent work up resulted in the isolation of two products, **1** (8%) and $[Ru_3(CO)_9(\mu\text{-}CO)(\mu_3\text{-}\eta^1,\eta^1,\eta^2\text{-}\{(C_5H_5)Fe(C_5H_4CCCHO)\})]$ **4** (30%). A single crystal grown from an *n*-hexane solution of **4**, was subjected to X-ray crystallographic analysis. The molecular structure of **4** in the solid-state is illustrated in Fig. 4 together with the atomic labelling scheme. Some important bond parameters are given in Table 4. The molecular structure of **4** is compatible with the EAN rule, which requires the presence of three Ru–Ru bonds [average 2.767(2) Å] and the alkyne to be a four-electron donor. This is bonded by two σ Ru–C bonds [Ru(1)–C(13) 2.09(1) Å, Ru(2)–C(11) 2.10(1) Å] and a π-coordination through C(11) and C(13) to Ru(3) [Ru(3)–C(11) 2.18(10) Å, Ru(3)–C(13) 2.34(9) Å]. This is different from that found in $[Ru_3(CO)_9(\mu\text{-}H)(\mu_3\text{-}\eta^1,\eta^2,\eta^2\text{-}CC\{(C_5H_4)Fe(C_5H_5)\})]$ [17] in which a σ Ru–C bond and two π-coordinations are involved. Thus, C(11)–C(13) is closely parallel to the Ru(1)–Ru(2) edge and the Ru_3C_2 skeleton can be regarded as having a *nido*-octahedral core geometry. Moreover, the Ru–bound alkyne bond length, C(11)–C(13), shows a characteristic lengthening to 1.38(1) Å, as expected for a μ_3-η^2 bound alkyne unit. The cyclopentadienyl rings are eclipsed and the ferrocene group is directed away from Ru(3) with the C_5H_4 ring closely coplanar with the Ru(1)–C(13)–C(11)–Ru(2) ring. This presumably maximises the pπ–pπ bonding in the C(13)–C(14) bond. The presence of the ferrocenyl group does not seem to lead to any noticeable distortion in the alkyne-to-metal cluster bonding. It should be noted that the aldehyde group is bent. This is attributed to the steric clash between the protons associated with C(15) of the C_5H_4 ring and the aldehyde carbon C(12). One carbonyl ligand, C(4)–O(4), bridges Ru(1) and Ru(2), while the other carbonyl ligands are normal terminal ligands which have Ru–C–O angles between 169 to 178°. There are only small differences in the coordination geometries of Ru(1) and Ru(2) due to the unsymmetrical arrangement of the bridging CO ligand. The spectroscopic data for compound **4** are fully consistent with its solid-state structure. The mass spectrum shows a parent peak at m/z 822 which is followed by the sequential loss of ten CO groups (Table 5). Its ^{1}H-NMR spectrum recorded in $CDCl_3$ displays two sets of triplets and one singlet in the range δ 4.40–4.09 for the nine protons of unsubstituted and substituted cyclopentadienyl rings, respectively. A downfield singlet signal at δ 10.15 due to the aldehyde proton is observed. The IR spectrum

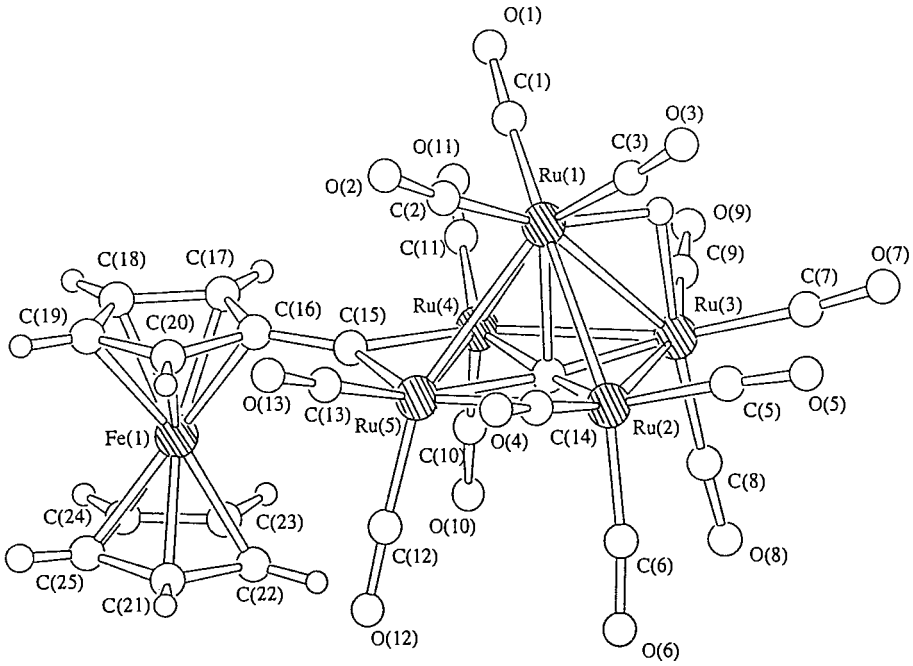

Fig. 3. Molecular structure of cluster **3**.

reveals six absorptions in the range of 2099–1860 cm^{-1}.

As far as the conformations of C_5H_5 and C_5H_4 rings of the ferrocenyl(formyl)acetylene group in compounds **1**–**4** are concerned, the eclipsed nature of the rings was confirmed by X-ray structural determination. The average distances of 1.64, 1.66, 1.65, and 1.65 Å from the centroids of the Cp ring to the iron atom in **1**, **2**, **3**, and **4**, respectively are recorded. The two rings of ferrocenyl(formyl)acetylene (C_5H_5 and C_5H_4) are almost parallel and eclipsed with a dihedral angle of 7.50, 4.60, 5.47 and 0.87° in clusters **1**, **2**, **3**, and **4**, respectively.

2.4. Electronic absorption spectra of ferrocenyl(formyl)acetylene, clusters 1–4

Table 6 presents the electronic spectral data for complexes **1**–**4** in CH_2Cl_2 at room temperature together with its starting material. A comparison of the spectra of ethynylferrocene [25] and ferrocenyl(formyl)acetylene indicates the presence of three bands ranging between 251 and 368 nm for the latter species. This may be due to electronic transitions involving orbitals based on the acetylenic aldehyde ($n \rightarrow \pi^*$ and $\pi \rightarrow \pi^*$). The reddish–orange colour of ferrocenyl(formyl)acetylene is due to the ferrocene moiety [λ_{max} (CH_2Cl_2) 468 nm, ε 1115 dm^3 mol^{-1} cm^{-1}]. The spectra of **1**–**4** in CH_2Cl_2 exhibit intense bands in the UV range 236–388 nm due to ligand-based $n \rightarrow \pi^*$ and $\pi \rightarrow \pi^*$ transitions as in the ligand, whereas four broad bands ranging from 462 to 573 nm are present in the visible region. We believe that these four low-energy bands are most likely a combination of absorption bands arising from both ferrocenyl and cluster fragments overlapping with each other.

2.5. Electrochemical properties of ferrocenyl(formyl)acetylene, cluster 1–4

The electrochemical properties of ferrocenyl(formyl)acetylene, clusters **1**–**4** have been studied by cyclic voltammetry at 298 K in a standard three-elec-

Table 3
Some selected bond lengths (Å) and angles (°) for cluster **3**

Bond lengths (Å)			
Ru(1)–Ru(2)	2.799(2)	Ru(1)–Ru(3)	2.857(2)
Ru(1)–Ru(4)	2.902(2)	Ru(1)–Ru(5)	2.940(2)
Ru(2)–Ru(3)	2.885(2)	Ru(2)–Ru(5)	2.922(2)
Ru(3)–Ru(4)	2.908(2)	Ru(4)–Ru(5)	2.640(2)
Ru(1)–C(14)	2.17(2)	Ru(2)–C(14)	2.00(2)
Ru(3)–C(14)	2.02(2)	Ru(4)–C(14)	2.00(2)
Ru(5)–C(14)	2.03(2)	Ru(4)–C(15)	1.95(2)
Ru(5)–C(15)	1.99(1)	Fe(1)–C(16)	2.03(2)
Fe(1)–C(17)	2.03(2)	Fe(1)–C(18)	2.03(2)
Fe(1)–C(19)	2.05(2)	Fe(1)–C(20)	2.03(2)
Fe(1)–C(21)	2.00(2)	Fe(1)–C(22)	2.08(2)
Fe(1)–C(23)	2.01(2)	Fe(1)–C(24)	2.04(2)
Fe(1)–C(25)	2.02(2)	C(15)–C(16)	1.42(2)
C(16)–C(17)	1.49(2)	C(16)–C(20)	1.41(2)
C(17)–C(18)	1.44(2)	C(18)–C(19)	1.36(3)
C(19)–C(20)	1.36(3)	C(21)–C(22)	1.42(3)
C(21)–C(25)	1.39(3)	C(22)–C(23)	1.37(3)
C(23)–C(24)	1.38(3)	C(24)–C(25)	1.38(2)
Bond angles (°)			
Ru(2)–Ru(3)–Ru(4)	87.1(5)	Ru(2)–Ru(5)–Ru(4)	91.6(6)
Ru(3)–Ru(4)–Ru(5)	93.1(6)	Ru(3)–Ru(2)–Ru(5)	87.9(5)

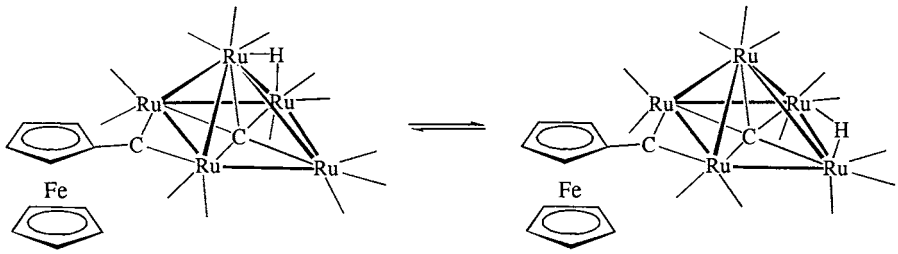

Scheme 2.

trode system with $[N^nBu_4][PF_6]$ in CH_2Cl_2 solution as the supporting electrolyte. The results are summarized in Table 7. Cyclic voltammetry of ferrocenyl-(formyl)acetylene revealed a quasi-reversible one-electron oxidation at 0.41 V which is slightly more anodic than that of the unsubstituted ferrocene and ethynylferrocene [39]. This denotes the electron-withdrawing ability of the acetylenic aldehyde group.

For compounds **1** and **4**, the ferrocenyl-based couple appears at $+0.47$ and $+0.50$ V respectively, which is slightly more anodic than those of the ferrocenyl-(formyl)acetylene. This indicates a poor electronic interaction between the metal core and the ferrocenyl fragment. Both compounds also exhibit two irreversible two-electron reduction processes. Compound **1** reveals an electrode potential for reduction of -0.99 V with an associated daughter peak at -0.25 V, whereas **4** presents a more negative potential of -1.18 V with two daughter peaks at $+0.09$ and $+0.5$ V. Cluster **2** shows two reversible one-electron oxidation process separated by ca. 190 mV. We assume that the first oxidation is based on the ferrocene moiety coordinated to the carbon bridging directly across the Ru–Ru bond. The positive shift of the oxidation with respect to ferrocenyl(formyl)acetylene is attributed to the electron-withdrawing ability of both the C≡C triple bond and the aldehyde group. By comparsion with the cyclic voltammogram of ferrocenyl(formyl)acetylene, which do not show any electrochemical processes within the potential window, the irreversible oxidation and reduction is confidently assigned to cluster-based processes. The cyclic voltammogram of **3** shows a chemically reversible ferrocenium–ferrocene couple at $+0.53$ V and an irreversible two electron reduction at -1.31 V with two daughter peaks at -0.57 and $+0.09$ V which is less cathodic than its parent cluster $[Ru_5C(CO)_{16}]$ [40].

3. Experimental

All the reactions were performed under an atmosphere of high-purity nitrogen using standard Schlenk techniques. Analytical grade solvents were purified by distillation over the appropriate drying agents and under an inert nitrogen atmosphere prior to use. Infrared spectra were recorded on a Bio-Rad FTS-7 spectrometer using a 0.5 mm solution cell. Positive-ion fast atom bombardment mass spectra were obtained using a Finnigan MAT 95 spectrometer. ^{1}H-NMR and ^{13}C-NMR spectra were recorded in $CDCl_3$ on a Bruker DPX 300 and DRX 500 NMR instrument, referenced to internal $SiMe_4$ ($\delta = 0$). The reactions were monitored by analytical TLC (5735 Kieselgel 60 F_{254}, E. Merck) and the products were separated on preparative thin-layer chromatographic plates coated with Merck Kieselgel 60 GF_{254}. Electronic absorption spectra were obtained with microprocessor-controlled Perkin–Elmer Lambda 3B UV–vis spectrophotometer using quartz

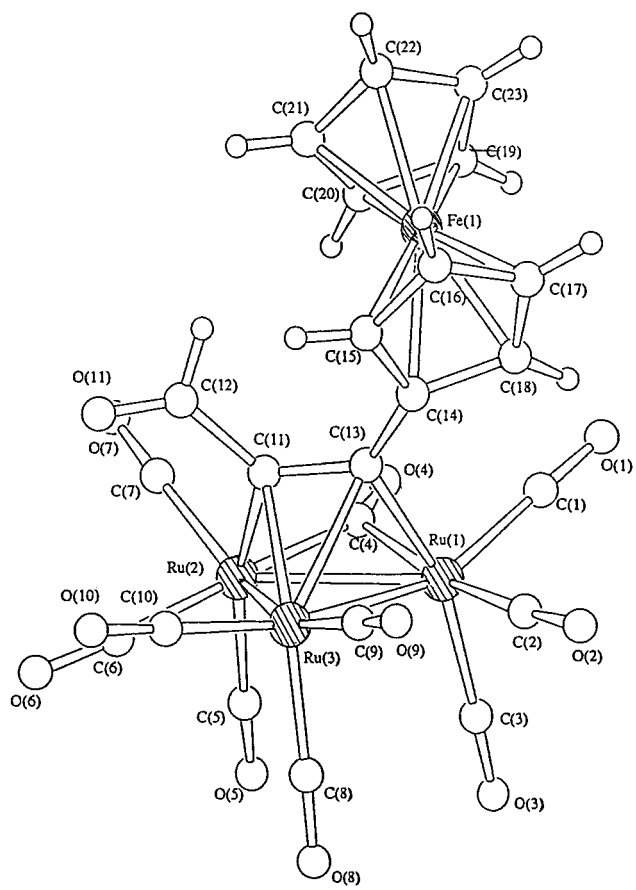

Fig. 4. Molecular structure of cluster **4**.

Table 4
Some selected bond lengths (Å) and angles (°) for cluster **4**

Bond lengths (Å)			
Ru(1)–Ru(2)	2.834(1)	Ru(1)–Ru(3)	2.737(1)
Ru(2)–Ru(3)	2.731(1)	Ru(1)–C(13)	2.09(1)
Ru(2)–C(11)	2.10(1)	Ru(3)–C(11)	2.18(10)
Ru(3)–C(13)	2.34(9)	Fe(1)–C(14)	2.07(1)
Fe(1)–C(15)	2.01(9)	Fe(1)–C(16)	2.04(1)
Fe(1)–C(17)	2.03(1)	Fe(1)–C(18)	2.03(1)
Fe(1)–C(19)	2.05(1)	Fe(1)–C(20)	2.02(1)
Fe(1)–C(21)	2.03(1)	Fe(1)–C(22)	2.04(1)
Fe(1)–C(23)	2.04(1)	C(11)–C(12)	1.48(2)
C(11)–C(13)	1.38(1)	C(13)–C(14)	1.45(2)
C(14)–C(15)	1.44(2)	C(14)–C(18)	1.44(1)
C(15)–C(16)	1.39(2)	C(16)–C(17)	1.40(1)
C(17)–C(18)	1.41(2)	C(19)–C(20)	1.40(2)
C(19)–C(23)	1.41(2)	C(20)–C(21)	1.38(2)
C(21)–C(22)	1.40(2)	C(22)–C(23)	1.39(2)
Bond angles (°)			
Ru(1)–Ru(2)–Ru(3)	58.8(3)	Ru(1)–Ru(3)–Ru(2)	62.4(3)
Ru(2)–Ru(1)–Ru(3)	58.6(3)	C(11)–Ru(3)–C(13)	35.3(4)

cells with a 1 cm path length. Voltammetric measurements were performed with a Princeton Applied Research (PAR) model 273A potentiostat connected to an interfaced computer. A standard three-electrode cell having a platinum wire counter electrode (Aldrich), and an $Ag \mid AgNO_3$ reference electrode (Bioanalytical) was employed. All measurements were carried out under an atmosphere of argon in anhydrous deoxygenated solvent. The compound ferrocenyl(formyl)acetylene was prepared according to methods described previously [41].

4. Synthesis

4.1. Reaction of $[Ru_3(CO)_{12}]$ with ferrocenyl(formyl)acetylene

The compound $[Ru_3(CO)_{12}]$ (0.100 g, 0.15 mmol) was stirred with ferrocenyl(formyl)acetylene (0.037 g, 0.15 mmol) in refluxing cyclohexane (30 ml) for 45 min. The solvent was removed in vacuo and the residue was separated by TLC using dichloromethane–hexane (1:1 v/v) as an eluent. This afforded two bands with R_f values of 0.45 and 0.60. Clusters **1** (R_f 0.45) and **2** (R_f 0.60) were isolated as solids in 20 and 10% yields, respectively. (Found for **1** $Ru_4FeC_{25}H_{10}O_{13}$: C, 30.83;

Table 6
The UV–vis spectral data for ferrocenyl(formyl)acetylene, clusters **1–4** [a]

Compound	λ_{max}/nm (ε/dm^3 mol^{-1} cm^{-1})
Ethynylferrocene	264 (8.1×10^3), 443 (0.22×10^3)
Ferrocenyl (formyl) acetylene	251 (8.5×10^3), 303 (1.0×10^4), 368 (1.7×10^3), 468 (1.1×10^3)
1	288 (4.1×10^4), 388 (1.4×10^4), 462 (8.8×10^3),
2	292 (2.6×10^4), 362 (1.8×10^4), 562 (4.6×10^3)
3	236 (3.7×10^4), 320 (1.5×10^4), 573 (4.0×10^3)
4	301 (3.4×10^4), 475 (4.5×10^3)

[a] In CH_2Cl_2.

Table 7
Electrochemical data for ferrocenyl(formyl)acetylene, clusters **1–4** in CH_2Cl_2 at 298 K [a]

Compound	$E_{1/2}$ (ΔE_p) [b]/V	Other oxidation/ V [c]	E_{pc}/V [c]
F(formyl) acetylene	0.41		
1	0.50		−0.99
2	0.32, 0.51	0.86	−1.26
3	0.53		−1.31
4	0.47		−1.18

[a] Obtained from dichloromethane solution containing 0.1 mol dm^{-3} [N^{n}Bu$_4$][PF$_6$] as the supporting electrolyte at a glassy carbon working electrode. All potentials quoted are vs. $Ag \mid AgNO_3$. Scan rate 100 mV s^{-1} at 25°C.

[b] Half-wave potential values $E_{1/2}$ refer to the ferrocenium–ferrocene couple.

[c] Irreversible wave.

Table 5
Spectroscopic data for clusters **1–4**

Cluster	IR, ν(CO) /cm^{-1} [a]	NMR, δ (J/Hz) [b]	MS, m/z [c]
1	2094w, 2070vs, 2042s, 2037vs, 2011m	10.87 (1H, s, H [a]), 4.31 (2H, t, $J=1.8$, C_5H_4), 4.22 (2H, t, $J=1.8$, C_5H_4), 4.17 (5H, s, C_5H_5)	979(979)
2	2079s, 2054vs, 2014vs, 1996w, 1987w, 1946w,	11.27 (1H, s, H [a]), 10.94 (1H, s, H [b]), 4.26–4.56 (4H, m, C_5H_4), 4.24 (5H, s, C_5H_5), 4.11–4.21 (4H, m, C_5H_4), 4.09 (5H, s, C_5H_5)	1004(1004)
3	2085m, 2052vs, 2037w, 2033vs, 2012m	5.41 (2H, s [d], C_5H_4), 5.27 (2H, s [d], C_5H_4), 4.34 (5H, s [d], C_5H_5), −21.39 (1H, s [d], RuH)	1080(1080)
4	2099s, 2068vs, 2056vs, 2033s, 2014s, 1855w	10.15 (1H, s, H [a]), 4.40 (2H, t, $J=1.7$, C_5H_4), 4.23 (5H, s, C_5H_5), 4.09 (2H, t, $J=1.7$, C_5H_4)	822(822)

[a] CH_2Cl_2.
[b] $CDCl_3$.
[c] Simulated values given in parentheses.
[d] Broad singlet.

H, 1.20. Anal. Calc.: C, 30.67; H, 1.03%. Found for **2** $Ru_3Fe_2C_{34}H_{20}O_{10}$: C, 40.94; H, 2.15. Anal. Calc.: C, 40.67; H, 2.01%.)

4.2. Thermolysis of 1

Compound **1** (0.05g, 0.05 mmol) was refluxed in toluene (30 ml) for 8 h. The solvent was removed in vacuo and the residue separated by TLC using dichloromethane–hexane (3:17 v/v) as an eluent to afford three bands. Cluster **3** (R_f 0.65) was isolated as a purple solid with a 10% yield. (Found for **3** $Ru_5FeC_{25}H_{10}O_{13}$: C, 27.93; H, 1.08%. Anal. Calc.: C, 27.80; H, 0.93%.)

4.3. Reaction of $[Ru_3(CO)_{10}(NCMe)_2]$ with ferrocenyl(formyl)acetylene

The compound $[Ru_3(CO)_{10}(NCMe)_2]$ [42] 0.085 g, 0.13 mmol) was stirred with ferrocenyl(formyl)acetylene (0.031 g, 0.13 mmol) in dichloromethane (60 ml) for 2 h at room temperature. Infrared spectroscopy and TLC indicated complete consumption of the starting material. The solvent was removed in vacuo and the residue was separated by TLC using dichloromethane–hexane (1:4 v/v) as the eluent to afford two bands with R_f values of 0.50 and 0.75. Cluster **4** (R_f 0.75) was isolated as an orange solid with a 30% yield. (Found for **4** $Ru_3FeC_{23}H_{10}O_{11}$: C, 33.78; H, 1.46%. Anal. Calc.: C, 33.64; H, 1.23%.)

5. X-ray data collection and structural determination of complexes 1–4

Crystals of all the new complexes suitable for X-ray analyses were mounted on top of a glass fibre using epoxy resin. Intensity data were collected at ambient temperature on either a Rigaku AFC7R diffractometer using a $\omega - 2\theta$ scan (for **1** and **3**) or MAR Research image plate scanner with ω scan technique (for **2** and **4**) with graphite-monochromated Mo–K_α radiation ($\lambda =$ 0.71073 Å). Crystal system and space group of the crystals were determined from Laue symmetry and systematic absences. A summary of the crystallographic data and structure refinement is listed in Table 8. All intensity data were collected for Lorentz and polarization effects. The Ψ-scan method was employed for semi-empirical absorption corrections for **1** and **3**, however, an approximation to absorption correction by

Table 8
Summary of crystal data and data collection parameters for clusters **1**–**4**

Cluster	**1**	**2**	**3**	**4**
Empirical formula	$Ru_4FeC_{25}O_{13}H_{10}$	$Ru_3Fe_2C_{35}H_{22}O_{10}Cl_2$	$Ru_5FeC_{25}H_{10}O_{13}$	$Ru_3FeC_{23}H_{10}O_{11}$
M	978.47	1088.36	1179.54	821.38
Crystal colour, habit	Red, rod	Red, rod	Red, plate	Red, plate
Crystal size (mm)	$0.21\times0.25\times0.29$	$0.13\times0.25\times0.26$	$0.26\times0.32\times0.35$	$0.25\times0.26\times0.31$
Crystal system	Monoclinic	Monoclinic	Monoclinic	Orthorhombic
Space group	$P2_1/c$ (no. 14)	$P2_1/c$ (no. 14)	$P2_1/c$ (no. 14)	*Pbca*
a (Å)	16.506(5)	15.240(1)	8.760(2)	9.741(1)
b (Å)	28.240(5)	7.922(1)	19.105(2)	14.656(1)
c (Å)	12.337(6)	29.557(1)	18.523(2)	35.486(1)
α (°)	90	90	90	90
β (°)	90.11(3)	90.90(2)	101.18(1)	90
γ (°)	90	90	90	90
V (Å^3)	5750(2)	3568(5)	3041.2(7)	5066.1(5)
Z	8	4	4	8
$D_{calc.}$ (g cm^{-3})	2.260	2.026	2.358	2.154
$F(000)$	3728	2120	2040	3152
μ (Mo–K_α) (cm^{-1})	26.11	22.41	29.48	23.75
2θ Range collected (°)	2.0–51.2	2.0–51.2	2.0–51.2	2.0–51.2
Reflections collected	8023	23665	4449	27551
Unique reflections	7713	4213	4134	3396
Observed reflections [$I>1.5\sigma(I)$]	4354	2251	2590	2002
R	0.061	0.063	0.059	0.049
R_w	0.077	0.058	0.062	0.042
Goodness-of-fit, S	2.34	1.36	1.63	1.51
Maximum Δ/σ	0.01	0.04	0.03	0.04
No. of variables	395	464	207	343
Maximum, minimum density in ΔF map close to Ru (e Å^{-3})	1.16, −1.06	1.64, −0.88	0.59, −0.45	1.04, −0.81

inter-image scaling was applied for **2** and **4**. Scattering factors were taken from Ref. 43(a) and anomalous dispersion effects 43b were included in F_c. The structures were solved by a combination of direct methods (SHELXS86 [44] for **3**; SIR88 [45] for **1**, **2** and **4**) and Fourier difference techniques and refined on F by full-matrix least-squares analysis. The hydrogen atoms of the organic moieties were generated in their ideal positions (C–H 0.95 Å). All calculations were performed on a silicon-graphics computer, using the program package TEXSAN [46].

6. Supplementary material

Additional material has been deposited with the Cambridge Crystallographic Data Centre (CCDC nos. 11749–11752) and comprises final atomic coordinates, thermal parameters and all bond parameters. Copies of this information may be obtained free of charge from The Director, CCDC, 12 Union Road, Cambridge, CB2 1EZ, UK (Fax: +44-1223-336-033; e-mail: deposit@ccdc.cam.ac.uk or www: htttp://www.ccdc.cam.ac.uk).

Acknowledgements

We gratefully acknowledge the financial support of this work by the Hong Kong Research Grants Council and the University of Hong Kong; C.S.-W.L. acknowledges the receipt of a postgraduate studentship administered by the University of Hong Kong.

References

[1] T.C. Zheng, W.R. Cullen, S.J. Rettig, Organometallics 13 (1994) 3549.
[2] W.Y. Wong, W.T. Wong, J. Chem. Soc. Dalton Trans. (1996) 3209.
[3] S.M. Lee, K.K. Cheung, W.T. Wong, J. Organomet. Chem. 502 (1996) 77.
[4] J.W.S. Hui, W.T. Wong, J. Chem. Soc. Dalton Trans. (1997) 2445.
[5] E. Sappa, A. Tiripicchio, P. Braunstein, Chem. Rev. 83 (1983) 203.
[6] E. Sappa, A. Tiripicchio, P. Braunstein, Coord. Chem. Rev. 65 (1985) 219.
[7] M.I. Bruce, A.G. Swincer, Adv. Organomet. Chem. 22 (1983) 59.
[8] C.V. Schnering, T. Albiez, W. Bernhardt, H. Vahrenkamp, Angew. Chem. Int. Ed. Engl. 25 (1986) 479.
[9] A.B. Antonova, A.A. Johansson, N.A. Deykhina, et al., Inorg. Chim. Acta 230 (1995) 97.
[10] C.S.W. Lau, W.T. Wong, J. Chem. Soc. Dalton Trans. (1998) 3391.
[11] C.S.W. Lau, W.T. Wong, J. Chem. Soc. Dalton Trans. (1999) 607.
[12] (a) L.T. Phang, S.C.F. Au-Yeung, T.S.A. Hor, S.B. Khoo, Z.Y. Zhou, T.C.W. Mak, J. Chem. Soc. Dalton Trans. (1993) 165. (b) M. Sato, H. Shintate, K. Kawata, M. Sekino, M. Katada, S. Kawata, Organometallics 13 (1994) 1956.
[13] (a) A. Togni, M. Hobi, G. Rihs, G. Rist, A. Albinati, P. Zanello, D. Zech, H. Keller, Organometallics 13 (1994) 1224. (b) S.B. Wilkes, I.R. Butler, A.E. Underhill, A. Kobayashi, H. Kobayashi, J. Chem. Soc. Chem. Commun. (1994) 53.
[14] (a) I.H. Williams, D. Spangler, D.A. Femec, G.M. Maggiora, R.L. Schowen, J. Am. Chem. Soc. 102 (1980) 6621. (b) D.C. Johnson, P.P. Edwards, R.E. Benfield, W.J.H. Nelson, M.D. Vargas, Nature (London) 314 (1985) 231. (c) A.J. Blake, A. Harrison, B.F.G. Johnson, E.J.L. McInnes, S. Parsons, D.S. Shephard, L.J. Yellowlees, Organometallics 14 (1995) 3160. (d) L.F. Dahl, W.L. Olsen, A.M. Stacy, J. Am. Chem. Soc. 108 (1986) 7646.
[15] J.J. Schneider, R. Goddard, C. Kröger, S. Werner, B. Metz, Chem. Ber. 124 (1991) 301.
[16] M.V. Russo, A. Furlani, S. Licoccia, R. Paolesse, A.C. Villa, C. Guastini, J. Organomet. Chem. 469 (1994) 245.
[17] A.A. Koridze, A.I. Yanovsky, Yu.T. Struchkov, J. Organomet. Chem. 441 (1992) 277.
[18] G.H. Worth, B.H. Robinson, J. Simpson, Organometallics 11 (1992) 501.
[19] A.J. Deeming, M.S.B. Felix, D. Nuel, N.I. Powell, D.A. Tocher, K.I. Hardcastle, J. Organomet. Chem. 384 (1990) 181.
[20] K.I. Hardcastle, A.J. Deeming, D. Nuel, N.I. Powell, J. Organomet. Chem. 375 (1989) 217.
[21] A.A. Koridze, V.I. Zdanovich, A.M. Sheloumov, V.Y. Lagunova, P.V. Peregudov, F.M. Dolgushin, A.I. Yanovsky, Organometallics 16 (1997) 2285.
[22] P.F. Jackson, B.F.G. Johnson, J. Lewis, P.R. Raithby, G.J. Will, M. McPartlin, W.J.H. Nelson, J. Chem. Soc. Chem. Commun. (1980) 1190.
[23] P. Mathur, S. Ghosh, M.M. Hossain, C.V.V. Satyanarayana, A.L. Rheingold, G.P.A. Yap, J. Organomet. Chem. 538 (1997) 57.
[24] H. Maatsuzaka, Y. Takagi, Y. Ishii, M. Nishio, M. Hidai, Organometallics 14 (1995) 2153.
[25] S.L. Ingham, B.F.G. Johnson, P.R. Raithby, K.J. Taylor, L.J. Yellowlees, J. Chem. Soc. Dalton Trans. (1996) 3521.
[26] R.D. Adams, I. Araf, G. Chen, J.C. Li, J.G. Wang, Organometallics 9 (1990) 2350.
[27] J.S. Song, G.L. Geoffroy, A.L. Rheingold, Inorg. Chem. 31 (1992) 1505.
[28] A.A. Koridze, N.M. Astakhova, F.M. Dolgushin, A.I. Yanovsky, Y.T. Struchkov, P.V. Petrovskii, Organometallics 14 (1995) 2167.
[29] M.I. Bruce, N.N. Zaitseva, B.W. Skelton, A.H. White, J. Organomet. Chem. 536 (1997) 93.
[30] J.S. Song, G.L. Geoffroy, A.L. Rheingold, Inorg. Chem. 31 (1992) 1505.
[31] C.J. Way, Y. Chi, I.J. Mavunkal, S.L. Wang, F.L. Liao, S.M. Peng, G.H. Lee, J. Cluster Sci. 8 (1997) 87.
[32] C.J. Adams, M.I. Bruce, N.J. Liddell, B.K. Nicholson, J. Organomet. Chem. 420 (1991) 105.
[33] D. Braga, F. Grepioni, B.F.G. Johnson, H. Chen, J. Lewis, J. Chem. Soc. Dalton Trans. (1991) 2559.
[34] B.F.G. Johnson et al., J. Chem. Soc. Dalton Trans. (1983) 277.
[35] S.L. Cook, J. Evans, L.R. Gray, M. Webster, J. Chem. Soc. Dalton Trans. (1986) 2149.
[36] A.G. Cowie, B.F.G. Johnson, J. Lewis, J.N. Nicholls, P.R. Raithby, M.J. Rosales, J. Chem. Soc. Dalton Trans. (1983) 2311.
[37] M.P. Diebold, S.R. Drake, B.F.G. Johnson, J. Lewis, M. McPartlin, H. Powell, J. Chem. Soc. Dalton Trans. (1988) 1358.
[38] R.D. Adams, Z. Li, J.C. Lii, W. Wu, Organometallics 11 (1992) 4001.

[39] D. Osella, O. Gambino, C. Nervi, M. Ravera, M.V. Russo, G. Infante, Inorg. Chim. Acta 225 (1994) 35.
[40] B.F.G. Johnson, J. Lewis, W.J.H. Nelson, J.N. Nicholls, J. Puga, P.R. Raithby, M.J. Rosales, M. Schröder, M.D. Vargas, J. Chem. Soc. Dalton Trans. (1983) 2447.
[41] G. Doisneau, G. Balavoine, T. Fillebeen-Khan, J. Organomet. Chem. 425 (1992) 113.
[42] A.J. Blake, P.J. Dyson, B.F.G. Johnson, C.M. Martin, J.G.M. Nairn, E. Parisini, J. Lewis, J. Chem. Soc. Dalton Trans. (1993) 981.
[43] D.T. Cromer, J.T. Waber, International Tables for X-Ray Crystallography, vol. 4 , Kynoch, Birmingham, 1974 (a) Table 2.2B, (b) Table 2.3.1.
[44] G.M. Sheldrick, SHELXS86, Program for crystal structure solution, Acta Crystallogr. Sect. A. 46 (1990) 467.
[45] M.C. Burla, M. Camalli, G. Cascarano, C. Giacovazzo, G. Polidori, R. Spagna, D. Viterbo, SIR88, J. Appl. Crystallogr. 22 (1989) 389.
[46] TEXSAN, Crystal structure analysis package, Molecular Structure Corporation, Houston, TX, 1985.